Supporting Information

Hierarchical Hybridization in Plasmonic Honeycomb Lattices

Ran Li,[†] Marc R. Bourgeois,[‡] Charles Cherqui,[‡] Jun Guan,[¶] Danqing Wang,[¶] Jingtian Hu,[†] Richard D. Schaller,[‡] George C. Schatz,[*,‡] and Teri W. Odom[*,†]

[†]*Department of Materials Science and Engineering*

[‡]*Department of Chemistry*

[¶]*Graduate Program in Applied Physics, Northwestern University, Evanston, Illinois 60208, United States*

E-mail: g-schatz@northwestern.edu; todom@northwestern.edu

List of Figures

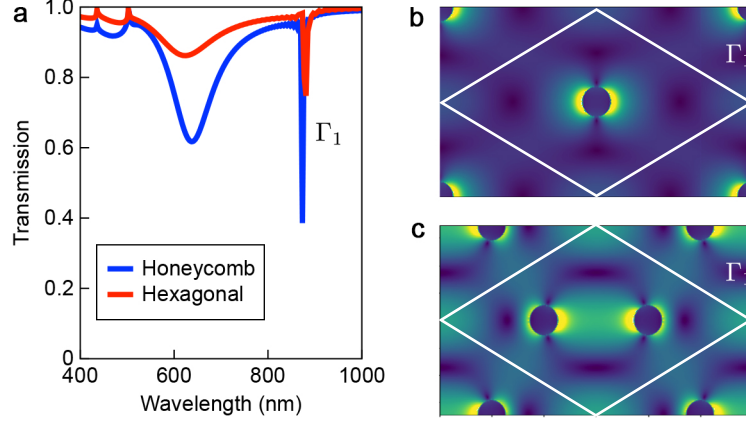Figure S1: Γ_1 SLR in hexagonal lattice. (a) Γ point x-polarized transmission spectra for honeycomb and hexagonal lattices calculated using FDTD. (b) Calculated electric field magnitude, normalized to that of the incident field, of Γ_1 SLR within the XY plane of hexagonal lattice unit cell. (c) Figure 1e of the main text reproduced for comparison with panel b).
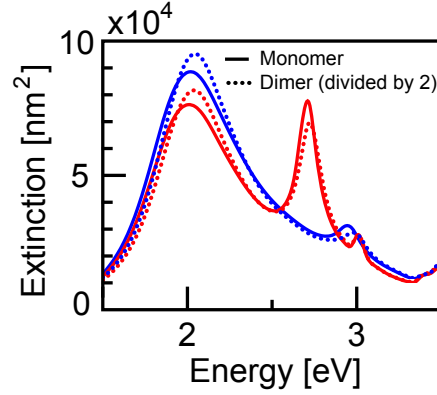
Figure S2: The spectral profiles of the Ag NP ($d = 110$ nm; $h = 50$ nm) dimer (dashed) closely match those of the isolated Ag NP (solid) after normalizing the former by a factor of 2 to account for the particle number. Deviations from the single-particle responses are small due to the 400 nm center-to-center distance between NPs in the dimer structure. The trace colors correspond to the plane wave excitation conditions in Figure 2 of the main text. Explicitly, red and blue traces correspond to incident plane waves polarized along short- and long-axes of the disc, respectively.
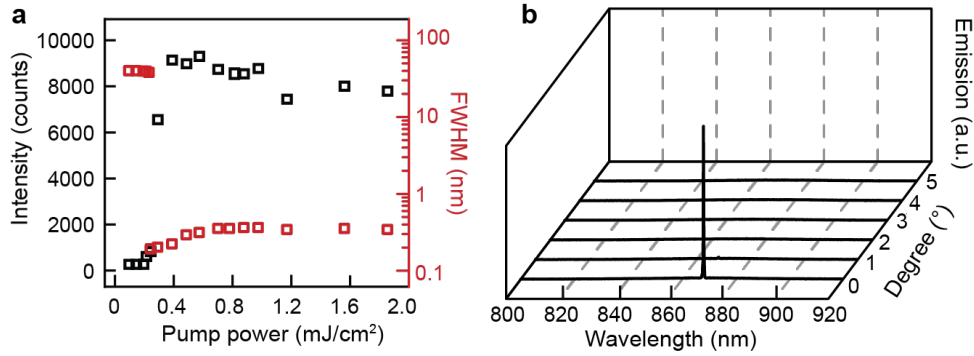

Figure S3: Γ_1 lasing characterization from Ag NP lattice. (a) Light-light curve of Γ_1 lasing and power-dependent emission FWHM. Lasing intensities and linewidths are plotted on linear and logarithmic scales, respectively. (b) Angle-resolved emission of Γ_1 lasing.
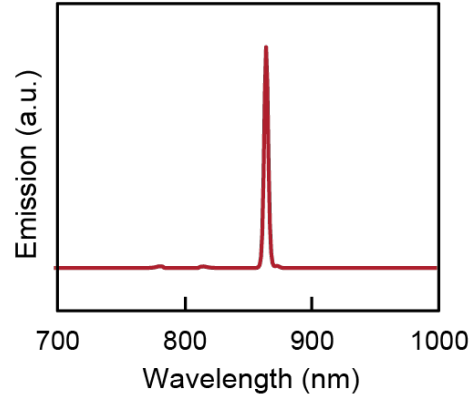
Figure S4: Simulated Γ_1 lasing emission peak matches wavelength of Γ_1 resonance in the absence of dye. Calculation details included in the main text.
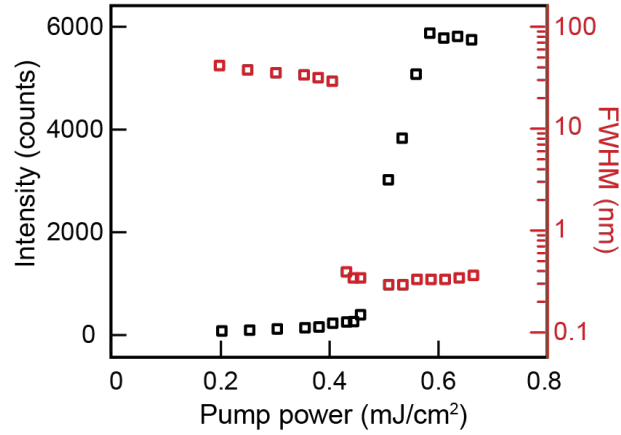

Figure S5: Lasing input-output curves suggesting the non-linear increase of intensity and threshold value of Al nanoparticle arrays. Lasing intensities are plotted on a linear scale. The power dependence of the emission FWHM is included in red on a logarithmic scale.
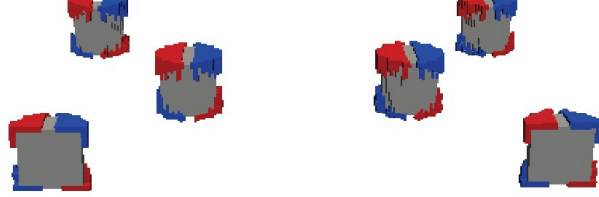
Figure S6: Surface charge distributions at Γ_2 resonance showing the charge accumulates at top and bottom surfaces of Al nanoparticles. Note that the two nearest and furthest NPs appear cut in half vertically since a rectangular region was simulated in FDTD using Bloch boundary conditions to produce these plots.
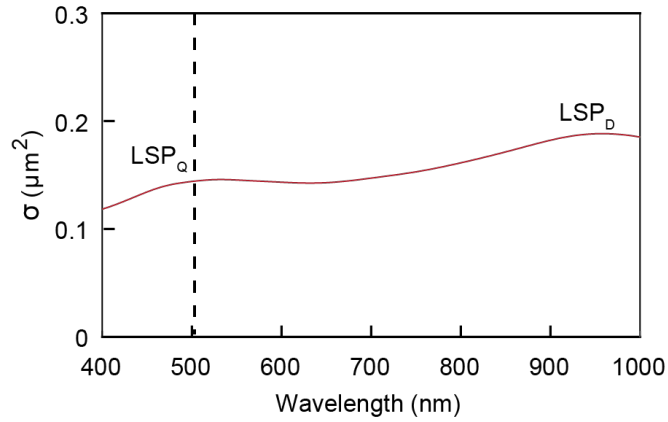

Figure S7: The Bragg mode associated with the Γ_2 resonance (denoted by the dash line) with the calculated scattering cross section of an isolated Al NP ($d = 110$ nm; $h = 100$ nm) in a medium with refractive index equal to 1.45. The spectral overlap between the out-of-plane quadrupole localized surface plasmon and the lattice Bragg mode facilitates the formation of the sharp Γ_2 lattice mode.
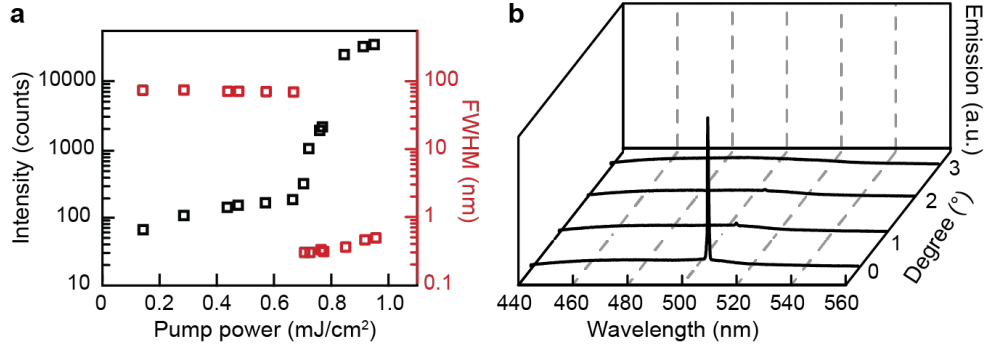
Figure S8: Light-light curve and angle-resolved emission suggested that Γ_2 lasing occurred at the Γ point ($k_{||} = 0$). (a) Input-output curves and power-dependent emission FWHM of Γ_2 lasing. Lasing intensities and linewidths are plotted on a logarithmic scale. (b) Angle-resolved emission spectra measured from 0° to 3°.